

LARGE FORMAT NARROW-BAND, MULTI-BAND, AND BROAD-BAND LWIR QWIP FOCAL PLANES FOR SPACE AND EARTH SCIENCE APPLICATIONS

S. D. Gunapala* and S. V. Bandara
Jet Propulsion Laboratory, Pasadena, CA 91109

ABSTRACT

A 640x512 pixel, long-wavelength cutoff, narrow-band ($\Delta\lambda/\lambda \sim 10\%$) quantum well infrared photodetector (QWIP) focal plane array (FPA), a four-band QWIP FPA in the 4-16 μm spectral region, and a broad-band ($\Delta\lambda/\lambda \sim 42\%$) QWIP FPA having 15.4 μm cutoff have been demonstrated.

I. INTRODUCTION

The QWIPs discussed in this article utilize the photoexcitation of electrons between the ground state and the first excited state in the conduction band quantum well. The quantum well structure is designed so that these photoexcited carriers can escape from the quantum well and be collected as photocurrent. These detectors afford greater flexibility than extrinsically doped semiconductor infrared detectors because the peak wavelength of the response, cutoff wavelength, and the spectral width of the response can be continuously tailored by varying layer thickness and barrier composition. There has been much interest lately¹ in large format QWIP focal plane arrays (FPAs). In this paper we discuss the design, fabrication, and test results of a 640x512 pixel narrow-band, four-band and broad-band QWIP FPAs in the 4-16 μm spectral region. These large format FPAs will be useful for many applications, such as the in-situ and remote sensing of gas molecules, thermal imaging, global atmospheric temperature profiles monitoring, cloud characteristics measurements, astronomy, tracking and identification of missiles, etc.

II. 640x512 PIXEL NARROW-BAND FOCAL PLANE ARRAY

Each period of the multi-quantum-well (MQW) structure consists of a 45 Å well of GaAs (doped $n = 5 \times 10^{17} \text{ cm}^{-3}$) and a 500 Å barrier of $\text{Al}_{0.3}\text{Ga}_{0.7}\text{As}$. Stacking many identical quantum wells together increases photon absorption. Ground state electrons are provided in the detector by doping the GaAs well layers with Si. This photosensitive MQW structure is sandwiched between 0.5 μm GaAs top and bottom contact layers doped $n = 5 \times 10^{17} \text{ cm}^{-3}$, grown on a semi-insulating GaAs substrate by molecular beam epitaxy (MBE). Then a 0.7 μm thick GaAs cap layer on top of a 300 Å $\text{Al}_{0.3}\text{Ga}_{0.7}\text{As}$ stop-etch layer was grown in-situ on top of the device structure to fabricate the light coupling optical cavity. The epitaxially grown material was processed into 200 μm diameter mesa test structures using wet chemical etching, and Au/Ge ohmic contacts were evaporated onto the top and bottom contact layers.

An experimentally measured responsivity spectrum is shown in Fig. 1. The responsivity of the detector peaks at 8.5 μm and the peak responsivity (R_p) of the detector is 83 mA/W at bias $V_B = -1.1 \text{ V}$. The spectral width and the cutoff wavelength are $\Delta\lambda/\lambda = 10\%$ and $\lambda_c = 8.9 \mu\text{m}$, respectively. The net peak quantum efficiency was 1.4% at bias $V_B = -1.1 \text{ V}$ for a 45° double pass. The lower quantum efficiency is due to the lower photoconductive gain at lower operating bias. Lower operating bias suppresses the dark current.

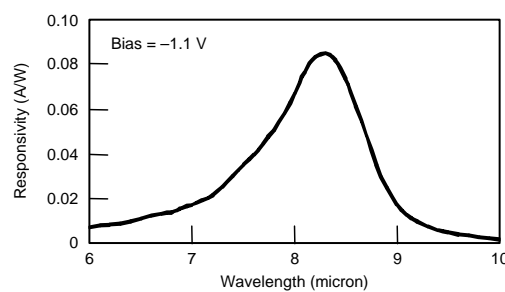


Figure 1. Responsivity spectrum of a bound-to-quasibound LWIR QWIP test structure at temperature $T = 77 \text{ K}$.

The photoconductive gain g was experimentally determined using¹ $g = i_n^2 / 4eI_D\Delta f + 1/(2N)$, where Δf is the measurement bandwidth, N is the number of quantum wells, and i_n is the current noise, which was measured using a spectrum analyzer. The photoconductive gain of the detector reached 0.98 at $V_B = -5 \text{ V}$. The peak detectivity is defined as $D_p^* = R_p \sqrt{A\Delta f} / i_n$, where R_p is the peak responsivity, A is the area of

*Contact information for S. D. Gunapala: Sarah.d.Gunapala@jpl.nasa.gov, phone (818) 354-1880

the detector and $A = 3.14 \times 10^{-4} \text{ cm}^2$. The measured peak detectivity at bias $V_B = -1.1 \text{ V}$ and temperature $T = 65 \text{ K}$ is $1 \times 10^{11} \text{ cm} \sqrt{\text{Hz}} / \text{W}$. Figure 2 shows the bias dependence of peak detectivity as a function of temperature. These detectors show BLIP at bias $V_B = -2 \text{ V}$ and temperature $T = 72 \text{ K}$ for a 300 K background with f/2 optics.

After the two-dimensional grating array was defined by the lithography and reactive ion etching, the photoconductive QWIPs of the 640x512 pixel FPAs were fabricated by dry etching through the photosensitive GaAs/ $\text{Al}_x\text{Ga}_{1-x}\text{As}$ multi-quantum well layers into the 0.5 μm thick doped GaAs bottom contact layer. The detector pixel pitch of the FPA is 25 μm and the actual pixel area is $23 \times 23 \mu\text{m}^2$. Indium bumps were then evaporated on top of the detectors for hybridization with a silicon readout integrated circuit (ROIC). QWIP FPAs were hybridized to a 640x512 pixel silicon CMOS readout and are biased at $V_B = -1.1 \text{ V}$. At temperatures below 72 K, the signal-to-noise ratio of the system is limited by array nonuniformity, readout multiplexer (i.e., ROIC) noise, and photocurrent (photon flux) noise. At temperatures above 72 K, the temporal noise due to the dark current becomes the limitation.

Figure 3 shows the measured NEDT histogram of the FPA at an operating temperature of $T = 65 \text{ K}$, 16 msec integration time, bias $V_B = -1.1 \text{ V}$ for 300 K background with f/2 optics, and the mean value is 20 mK. This agrees reasonably well with our estimated value of 10 mK based on test detector data. The net peak quantum efficiency of the FPA was 1.5%, which also agrees closely with the single element test detector results. It is worth noting that under BLIP conditions the performance of the detectors is independent of the photoconductive gain, and depends only on the absorption quantum efficiency.

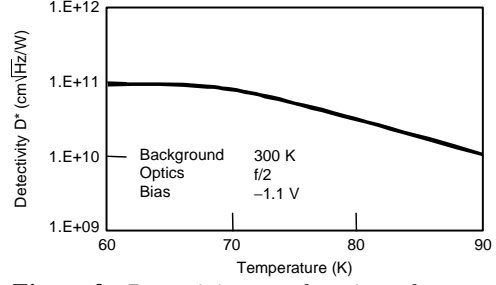


Figure 2. Detectivity as a function of temperatures at bias of -1.1 V .

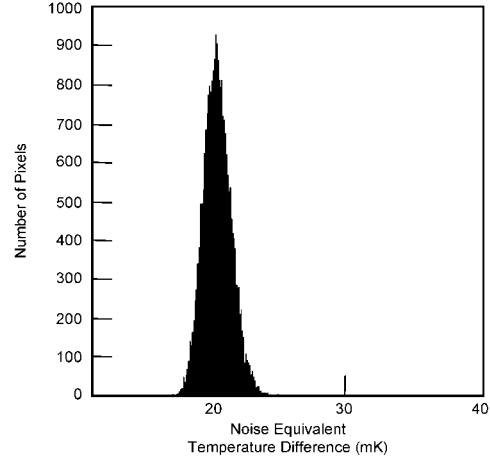


Figure 3. NEDT histogram of the 327,680 pixels of the 640x512 array showing a high uniformity of the FPA.

III. 640X512 PIXEL FOUR-COLOR SPATIALLY SEPARATED FOCAL PLANE ARRAY

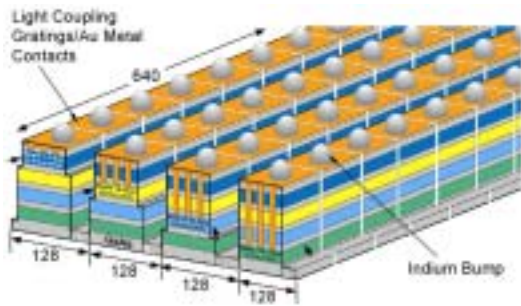


Figure 4. Layer diagram of the four-band QWIP device structure and the deep groove two-dimensional periodic grating structure. Each pixel represent a 640x128 pixel area of the four-band focal plane array.

structure is dominated by the longest wavelength portion of the device structure, the VLWIR QWIP structure has been designed to have a bound-to-quasibound intersubband absorption peak at 14.0 μm . Other QWIP device structures have been designed to have a bound-to-continuum intersubband absorption process because the photo current and dark current of these devices are relatively small compared to the VLWIR device. This whole four-band QWIP device structure was then sandwiched between 0.5 μm GaAs

This four-band vertically integrated device structure was achieved by the growth of multi-stack QWIP structures separated by heavily doped n^+ contact layers, on a GaAs substrate. Device parameters of each QWIP stack were designed to respond in different wavelength bands. Figure 4 shows the schematic device structure of a four-color QWIP FPA. A typical QWIP stack consists of a MQW structure of GaAs quantum wells separated by $\text{Al}_x\text{Ga}_{1-x}\text{As}$ barriers. The actual device structure consists of a 15 period stack of 4-5 μm QWIP structure, a 25 period stack of 8.5-10 μm QWIP structure, a 25 period stack of 10-12 μm QWIP structure and a 30 period stack of 13-15.5 μm QWIP structure. Each photosensitive MQW stack was separated by a heavily doped n^+ (thickness 0.2 to 0.8 μm) intermediate GaAs contact layer (see Fig. 4). Since the dark current of this device

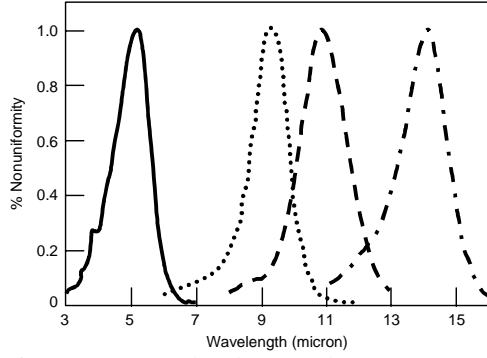


Figure 5. Normalized spectral response of the four-band QWIP FPA.

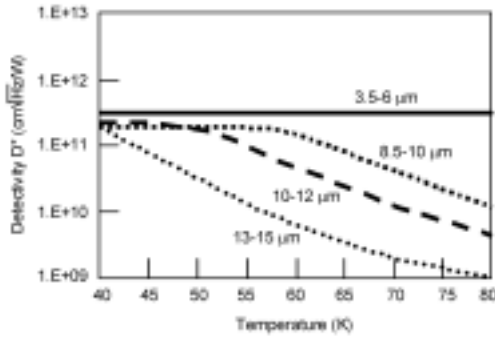


Figure 6. Detectivities of each spectral-band of the four-band QWIP FPA as a function of temperature.

12, 10-12, and 13.5-15.5 μm spectral bands show BLIP at temperatures 40, 50, 60 and 120 K, respectively, for a 300 K background with a $f/5$ cold stop. As expected (due to BLIP), the estimated and experimentally obtained NEDT values of all spectral-bands do not change significantly below their BLIP temperatures. The experimentally measured NEDT of 4-5, 8-12, 10-12, and 13.5-15.5 μm detectors at 40 K are 21.4, 45.2, 13.5, and 44.6 mK, respectively. These experimentally measured NEDT agree reasonably well with the estimated NEDT values based on the single element test detector data¹.

IV. 640x512 PIXEL BROAD-BAND QWIP FOCAL PLANE ARRAY

The broadband QWIP device structure was designed by repeating a unit of several quantum wells with slightly different parameters such as well width and barrier height¹. The positions of ground and excited states of the quantum well are determined by the quantum well width (L_w) and the barrier height, i.e. the Al mole fraction (x) of the barrier. Since each single set of parameters for a bound-to-quasibound quantum well¹ corresponds to a spectral band pass of about 1.5 μm , three different sets of values are sufficient to cover a 10-16 μm spectral region (see Fig. 18). The MQW structure consists of many periods of these three-quantum-well units separated by thick barriers¹.

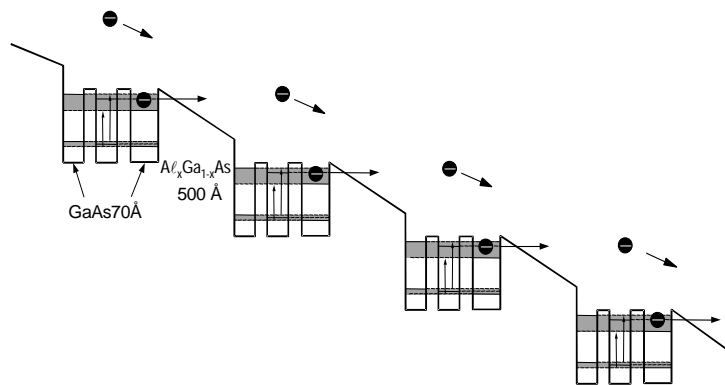


Figure 7. Broad-band MQW structure is designed by repeating a unit of several quantum wells with slightly different parameters such as well width and barrier height.

top and bottom contact layers doped with $n = 5 \times 10^{17} \text{ cm}^{-3}$ and was grown on a semi-insulating GaAs substrate by MBE.

In this section, we discuss the demonstration of the first 640x512 pixel monolithic spatially separated four-band QWIP FPA. The unique feature of this spatially separated four-band FPA is that the four infrared bands are independently and simultaneously readable on a single imaging array. This feature leads to a reduction in instrument size, weight, mechanical complexity, optical complexity and power requirements since no moving parts are needed. Furthermore, a single optical train can be employed, and the whole focal plane can operate at a single temperature.

The individual pixels of the four-color FPA were defined by photolithographic processing techniques (masking, dry etching, chemical etching, metal deposition, etc.). Four separate detector bands were defined by a deep trench etch process and the unwanted spectral bands were eliminated by a detector short-circuiting process. The unwanted top detectors were electrically shorted by gold-coated reflective two-dimensional etched gratings as shown in the Fig. 4. In addition to shorting, these gratings serve as light couplers for active QWIP stack in each detector pixel¹. Design and optimization of these two-dimensional gratings to maximize QWIP light coupling are extensively discussed elsewhere¹. The unwanted bottom QWIP stacks were electrically shorted at the end of each detector pixel row. Figure 6 shows the peak detectivities of all four spectral-bands as a function of operating temperature. Based on this single element test detector data, the 4-5, 8-

The device structure reported here involved 33 repeated layers of GaAs three-quantum-well units separated by $L_B \sim 575 \text{ \AA}$ thick $\text{Al}_x\text{Ga}_{1-x}\text{As}$ barriers. The well thickness of the quantum wells of three-quantum-well units are designed to respond at peak wavelengths around 13, 14, and 15 μm , respectively. These wells are separated by $L_u \sim 75 \text{ \AA}$ thick $\text{Al}_x\text{Ga}_{1-x}\text{As}$ barriers. The Al mole fraction (x) of barriers throughout the structure was chosen such that the $\lambda_p = 13 \mu\text{m}$ quantum well operates under bound-to-quasibound conditions. The excited state energy level broadening has been further enhanced due to the overlap of the wavefunctions associated with excited states of quantum wells separated by thin barriers¹. Energy band calculations based on a two band model show excited state energy levels spreading about 28 meV.

In Fig. 8, the responsivity curve at $V_B = -2.5 \text{ V}$ bias voltage shows broadening of the spectral response up to $\Delta\lambda \sim 5.5 \mu\text{m}$, (i.e. the full-width at half-maximum from 10.5 – 16 μm). This broadening $\Delta\lambda/\lambda_p \sim 42 \%$ is about a 400% increase compared to a typical bound-to-quasibound QWIP. The responsivity of the detector peaks at 13.5 μm and the peak responsivity (R_p) of the detector is 250 mA/W at bias $V_B = -2.5 \text{ V}$. The peak quantum efficiency was 11% at bias $V_B = -2.5 \text{ V}$ for a 45° double pass. The calculated D^* value for the present device ($\lambda = 15.4 \mu\text{m}$) at $T = 55 \text{ K}$ and $V_B = 2.5 \text{ V}$ is $3 \times 10^{10} \text{ cm}^2/\text{Hz}/\text{W}$. Even with broader response, this D^* is comparable to previously reported D^* of QWIPs with narrow spectral response. Figure 9 shows the detectivity D^* as a function of the operating temperature of the device. A light coupling random reflector array was defined by the lithography and dry etching. Photoconductive QWIPs of the 640x512 pixel FPAs were then fabricated by dry etching through the photosensitive GaAs/ $\text{Al}_x\text{Ga}_{1-x}\text{As}$ MQW layers into the 0.5 μm thick doped GaAs bottom contact layer. The pixel pitch of the FPA is 25 μm and the actual pixel size is $23 \times 23 \mu\text{m}^2$. The random reflectors on top of the detectors were then covered with Au/Ge and Au for Ohmic contact and reflection. Indium bumps were then evaporated on top of the detectors for hybridization with silicon ROIC. A single QWIP FPA was chosen and hybridized to a 640x512 pixel silicon CMOS ROIC and biased at $V_B = -2.5 \text{ V}$. At temperatures below 48 K, the signal to noise ratio of the system is limited by array nonuniformity, multiplexer readout noise, and photo current (photon flux) noise.

In summary, we have demonstrated the first 640x512 pixel spatially separated monolithic four-band FPA, narrow-band FPA, and the first 640x512 pixel broad-band FPA. These can be used in many ground based and space borne applications that require long-wavelength, large, uniform, reproducible, and low 1/f noise narrow-band, multi-band, and broad-band LWIR FPAs. These FPAs were back-illuminated through the flat thinned substrate membrane (thickness $\approx 2000 \text{ \AA}$). As described elsewhere¹ this thinned GaAs FPA membrane has completely eliminated the thermal mismatch between the silicon CMOS ROIC and the GaAs based QWIP FPA, and has completely eliminated the pixel-to-pixel optical cross-talk of the FPA. This initial array gave very good images with 99.9% operability.

ACKNOWLEDGMENTS

The research described in this paper was performed by the Jet Propulsion Laboratory, California Institute of Technology, and was jointly sponsored by the Breakthrough Sensors and Instrument Component Technology Thrust of the NASA Cross-Enterprise Technology Development Program and the Advance Technology Initiative Program of the NASA Earth Science Technology Office.

REFERENCES

- 1 S. D. Gunapala and S. V. Bandara, *Quantum Well Infrared Photodetector (QWIP) Focal Plane Arrays*, Semicon. Semimet., vol. 62, H. C. Liu and F. Capasso, Ed. San Diego: Academic Press, pp. 197-282, 2000.

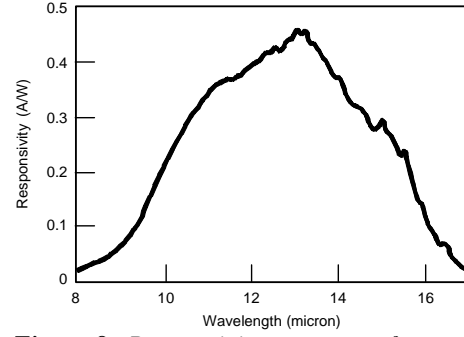


Figure 8. Responsivity spectrum of a broadband QWIP at temperature $T = 55 \text{ K}$.

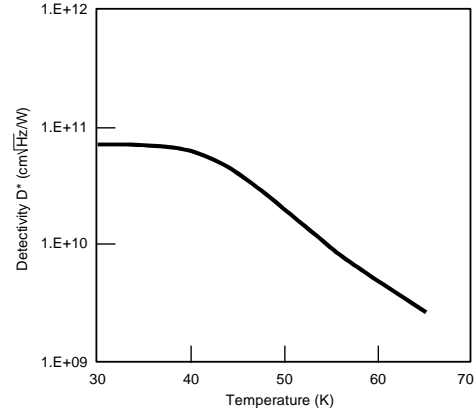


Figure 9. Detectivity as a function of temperatures at bias voltage $V_B = -2.5 \text{ V}$.